Magnetotransport and magnetoresistance properties of $Pr_{0.68}Ca_{0.32-x}Sr_xMnO_3$ (x= 0, 0.1, 0.18, 0.26 and 0.32) manganites

T. IZGI, V. S. KOLAT, N. BAYRI, A. O. KAYA, H. GENCER*, S. ATALAY
Inonu University, Science and Arts Faculty, Physics Department 44069 Malatya, Turkey

In this study, the magnetotransport and magnetoresistance properties of $Pr_{0.68}Ca_{0.32-x}Sr_xMnO_3$ (x= 0, 0.1, 0.18, 0.26 and 0.32) compounds were investigated. The system illustrate an evolution from a charge-ordered manganite at x = 0, with an insulating-like resistivity and low magnetization values, towards to a completely ferromagnetic metallic state for x = 0.32. Above the metal-insulator transition temperature T_{MI}, the resistance curves were fitted to the small polaron popping model. The activation energy (E_a) was found to decrease with increasing Sr content. In the phase separated (PS) state, due to the coexistence of ferromagnetic (FM) metallic and charge order (CO) insulating phases, the magnetoresistance (MR) was found to be maximum. The MR ratio of $6.3x10^8$ for the sample x = 0 at 60 K is one of the largest MR change has been reported in manganites. The MR values decreases considerably with increasing Sr content and the activation energy decreases with the increase of Sr content

(Received November 24, 2011; accepted June 9, 2011)

Keywords: Manganites, Colossal magnetoresistance, Transport and magnetic properties, Metal-insulator transition,

1. Introduction

Mixed valent perovskite manganites with the general formula $R_{1-x}A_xMnO_3$ (R = rare-earth cation, A = alkali-metal or alkaline-earth cation) have been extensively studied due to the colossal magnetoresistance (CMR) and magnetocaloric (MC) properties which offer potential applications such as read or write heads in magnetic recording media, sensors, electronic materials and refrigeration technology [1-8]. In the manganites, the charge, spin, orbital and lattice degrees of freedom are strongly coupled together and lead to a rich variety of phases with different physical properties such as ferromagnetic metallic (FM-M), antiferromagnetic insulator (AFM-I), charge ordering (CO), orbital ordering (OO), polaron formation and phase separation [9-11]. The origin of FM, AFM and the electrical conductivity in manganites is directly connected to the double-exchange (DE) mechanism, in which the electronic conduction is connected to ferromagnetic interactions between Mn^{3+} and Mn^{4+} cations via intermediate oxygen atoms [12]. The DE mechanism and MR have been related to the Mn^{3+}/ Mn^{4+} ratio, strong electron-phonon coupling due to the Jahn-Teller effect [13]. It is also clear that the lattice strain and structural deformations governed by the mean radii of A-site or B-site cations, which affect the $Mn3^{+}$-O-Mn^{4+} bond angle and bond length, have dramatic consequences on the transport and MR properties of these systems [14].

Recently, it has been reported that the manganites present a huge CMR generally have a phase separated state (PS) [15-18]. In PS state a chemically homogeneous material forms a magnetically inhomogeneous system with spatially coexisting regions with distinct magnetic and electronic properties such as simultaneous coexistence of submicrometer FM metallic and CO-AFM insulating regions. Previous works have reported this phenomenon in different compound of manganites, changing $<r_A>$ and the doping level [19-21]. The phase-separated state is closely related with the competition between antiferromagnetic CO insulating and FM metallic phases. The application of a magnetic field leads to metamagnetic transition (MMT) by increasing the FM region. At that point the resistivity decreases several order and induces a huge enhancement of MR [22, 23].

Pr-based manganites have been extensively studied due to the numerous remarkable properties like AFM-FM phase transition, CO, PS and MMT [24-30]. In $Pr_{0.65}Ca_{0.35}MnO_3$, the substitution of Ca^{2+} with the bigger Sr^{2+} ions provokes an increase of $<r_A>$, changing the properties of the system from CO to fully FM state for $Pr_{0.65}Sr_{0.35}MnO_3$ [7]. In the case of $Pr_{0.65}Ca_{0.35-x}Sr_xMnO_3$, the occurrence of PS, involving FM metallic and AFM-CO insulating regions are observed [18, 31]. As discussed above, in the PS region, application of a magnetic field leads to metamagnetic transition by increasing the FM region. This behavior induces a considerable decrease in resistivity and a huge enhancement of MR [23]. Therefore, in Pr-based manganites, transports, magnetic and PS-induced huge enhancement of magnetoresistance properties have been extensively investigated. [8, 28, 32-35].

A high value of the CMR in these compounds was reported by Maignan et al. [32] that $Pr_{0.7}Sr_{0.04}Ca_{0.26}MnO_3$ exhibited an MR ratio of 10^{11} by applying a magnetic field of 5T at 30 K, which was close to the upper limit of the CMR that can be reached in these compounds. Later,

Hejtmanek et al. [33] explained the CMR effects in the PrCaSrMnO thin films by the paramagnetic–antiferromagnetic and antiferromagnetic– ferromagnetic transitions which exist in these thin films. Mollah et al. [34, 35], explained the electronic, magnetic and thermal properties of polycrystalline $Pr_{0.65}Ca_{0.35-x}Sr_xMnO_3$ (x = 0-0.35) and they observed a huge enhancement of MR (99% at H = 0.5 T) for x = 0.1 sample. Wu at al. [28] showed a magnetoresistance ratio of > 10^{10} in a 2 T magnetic field for $Pr_{0.65}(Ca_{0.75}Sr_{0.25})_{0.35}MnO_3$ single crystal sample. Liu et al. [36] calculated the large value of MR (2400% at 5.5 T) for $Pr_{0.7}Sr_{0.05}Ca_{0.25}MnO_3$ thin film.

As discussed above, in most of the previous studies on Pr-based manganites, magnetoresistance properties were mostly reported for low Sr doping level especially in film and single crystal structure forms and there has not been any systematic report about magnetoresistance properties for $Pr_{0.68}Ca_{0.32-x}Sr_xMnO_3$ (x = 0, 0.1, 0.18, 0.26 and 0.32) compounds particularly in polycrystalline form. Previously we have detailed studied the magnetic and magnetocaloric properties of the same compounds [8]. In this article we report magnetotransport and magnetoresistance properties of $Pr_{0.68}Ca_{0.32-x}Sr_xMnO_3$ (x = 0, 0.1, 0.18, 0.26 and 0.32) polycrystalline compounds in detail.

2. Experimental

The polycrystalline $Pr_{0.68}Ca_{0.32-x}Sr_xMnO_3$ (x=0, 0.1, 0.18, 0.26 and 0.32) compounds were prepared by the conventional solid-state reaction using high purity powders Pr_6O_{11}, $SrCO_3$, $CaCO_3$, MnO. The powders were mixed in stoichiometric ratio. Thoroughly mixed powders were grounded and calcined in air at 800 °C for 10 h. After grinding, the mixed powders were pressed into a disk-shape with a diameter of 13 mm and a thickness of about 2 mm. The disk samples were first sintered at 1200 °C for 24 h in air. For good crystallization, this sintering, grinding and pelleting process was repeated three times. Final sintering was performed at 1350 ºC for 24 h in air. All the samples were cooled to room temperature at a cooling rate of 3 ºC/min.

The X-ray diffractograms were recorded with a power diffractometer at room temperature using Cu-Kα radiation. Grain structure was observed using a LEO-EVO-40 scanning electron microscope. The magnetic measurements were performed using a Q-3398 (Cryogenic) magnetometer in a temperature range from 5 to 300 K and 6T maximum magnetic field was applied. The magnetic entropy, which is associated with the magnetocaloric effect, can be calculated from the isothermal magnetization curves under the influence of a magnetic field.

3. Results and discussion

As detailed discussed in our previous study, the X-ray results of the $Pr_{0.68}Ca_{0.32-x}Sr_xMnO_3$ (x= 0, 0.1, 0.18, 0.26 and 0.32) samples have showed that all the samples have a single phase of orthorhombic symmetry [8]. Based on the XRD pattern, the unit cell parameters were calculated for $Pr_{0.68}Ca_{0.32-x}Sr_xMnO_3$ samples. The results have showed that all the orthorhombic unit cell parameters a, b and c increase slightly as the A-site cation varies from Ca^{2+} (1.18 A^0) to Sr^{2+} (1.31 A^0) [8]. The observed increase in unit cell parameters is concluded as the substitution of a large ion (Sr^{2+}) expands the unit cell in all the three direction (a, b and c). The typical SEM micrograph for $Pr_{0.68}Ca_{0.22}Sr_{0.1}MnO_3$ sample reflects a smooth polycrystalline structure with the grain size is 20-60 μm [8].

Fig. 1 shows the temperature dependence of resistance for the $Pr_{0.68}Ca_{0.32-x}Sr_xMnO_3$ (x = 0, 0.1, 0.18, 0.26, 0.32) samples at very low magnetic field (0.1 T). As can be seen from Fig.1, while the sample for x = 0 ($Pr_{0.68}Ca_{0.32}MnO_3$) shows insulating character, the sample for x = 0.32 ($Pr_{0.68}Sr_{32}MnO_3$) displays a fully metallic character at all the temperature range. The change from CO-AFM insulating phase for x = 0 sample to FM metallic phase for x = 0.32 sample is clearly seen. The samples for x = 0 and 0.1 demonstrate the insulating behavior at all the temperature range. The metal-insulator transition (MI) transition in $Pr_{0.68}Ca_{0.32-x}Sr_xMnO_3$ is observed for $x \geq 0.18$ at very low magnetic field. While the samples for x = 0.18-0.32 reveal insulating behavior first and than followed by a metallic character due to the MI transition with decreasing temperature. The MI transition temperature (T_{MI}) increases from 218 K for x=0.18 sample to 280 K for x = 0.32 sample with the increase of x.

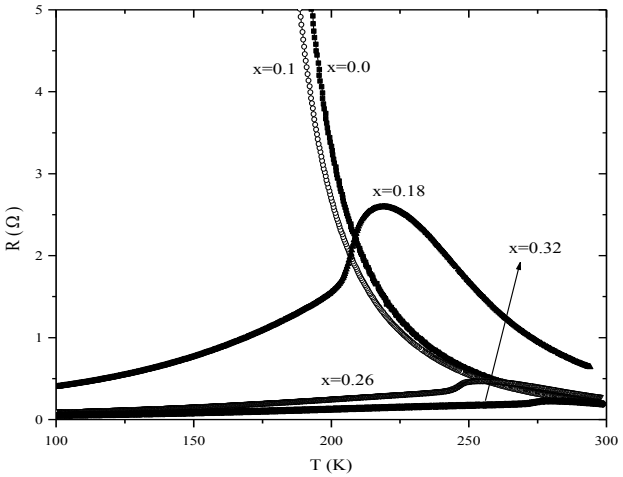

Fig. 1The temperature dependence of resistance for the $Pr_{0.68}Ca_{0.32-x}Sr_xMnO_3$ (x = 0, 0.1, 0.18, 0.26, 0.32) samples at low magnetic field (0.1 T).

Fig. 2 (a-e) shows the temperature dependence of resistance for the $Pr_{0.68}Ca_{0.32-x}Sr_xMnO_3$ (x = 0, 0.1, 0.18, 0.26, 0.32) samples at various magnetic fields. It is clearly seen from Fig. 2, when the samples are cooled from 300 K to lower temperatures, the resistance first increases to a maximum peak value and then followed by a sharp decrease due to the rapid growth of FMM phase fraction at

the expense of the CO phase. However, at low magnetic fields (H < 3T), the resistances curve of the sample for x = 0 shows an anomaly at lower temperatures. With increasing temperature, the system becomes unblocked due to the thermal fluctuation which is accompanied by a slight decrease in resistance near 45 K (Fig.2 a). This fact was also observed in magnetization curves near 45 K [8]. For the higher temperature value (between 50 and 100 K) a sharp increase in resistance was observed. In the previous studies [24-31, 37] it has been concluded that this corresponds to a transition back to the CO insulating dominated phase as the temperature is increased. As can be seen from Fig 2 (a), the observed resistance anomaly at lower temperatures disappeared at 3 T magnetic field. This clearly illustrates that the applied magnetic field favors melting of CO insulating state and an increase in the FM metallic phase fraction. For the samples x = 0.18, 0.26 and 0.32, the resistance curves behave such a full FM material (Fig. 2 c-e). All the samples show metal-insulator transition occurs at T_{MI} 218 K, 254 K and 280 K for x = 0.18, 0.26 and 0.32 respectively at zero magnetic field. It is clear that the MI transition temperature (T_{MI}) increases with increasing magnetic field. Fig.2 also shows that the resistance value monotonically decreases with increasing Sr-doping level. There is a huge decrease in the resistance value of the samples for x = 0.18, 0.26 and 0.32 compared with x = 0 sample (from $6.6x10^5$ Ω for x = 0 to 0.22 Ω for x = 0.32). Another important point is that the variation of resistance with magnetic field considerably decreases with increasing Sr-content.

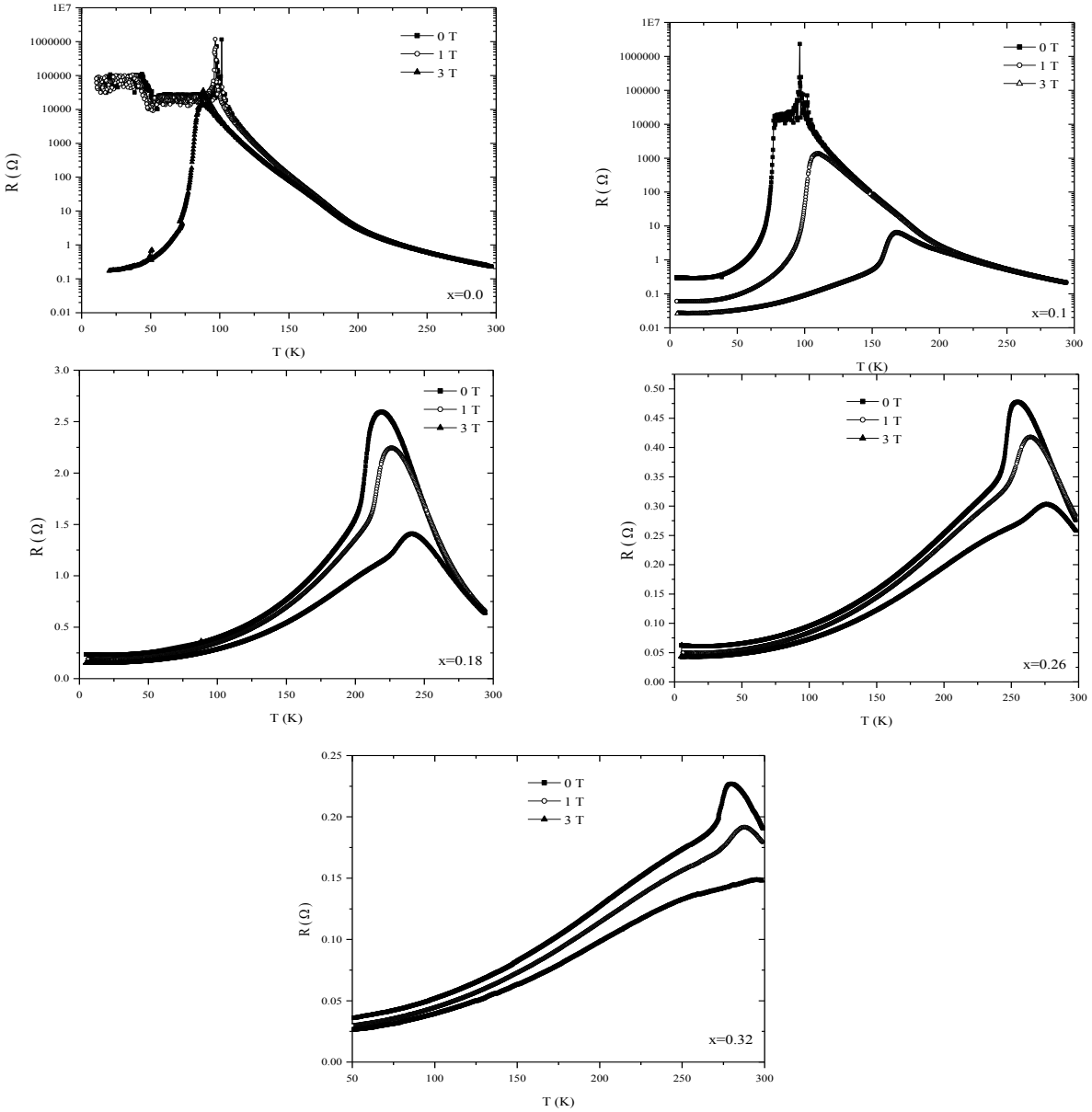

Fig. 2 The temperature dependence of resistance for the $Pr_{0.68}Ca_{0.32-x}Sr_xMnO_3$ samples of (a) x = 0, (b) x = 0.1, (c) x = 0.18, (d) x = 0.26 and (e) x = 0.32 at various magnetic fields.

The recent several experimental works [15-21] have reported that in different phase-separated perovskite manganites the relation between the transport and magnetic properties and the competition between the different interactions are close related with $<r_A>$. It has been showed that for a given carrier concentration the strongest CO states are found for the lowest $<r_A>$ values. When the CO state is established, the resistance turns to strong insulating behavior as in the case of x = 0 and 0.1 samples. In many studies on the perovskite manganites, it has been showed that the replacement of A-site ions with others which have different size and oxidation state can cause two main changes in materials. One is Mn^{3+}/Mn^{4+} ratio and the other is the structural change because a change in Mn-O bond length or Mn-O-Mn bond angle [38]. When Ca^{2+} ions are substituted by Sr^{2+} ions, the Mn^{3+}/Mn^{4+} ratio and hence the hole density in the system unchanged due to the same oxidation state of Ca^{2+} and Sr^{2+}. The only effect originates from the difference of the atomic size of the Ca^{2+} (1.18 A^0) and Sr^{2+} (1.31 A^0) ions. When Ca^{2+} ions are substituted by Sr^{2+} ions which have larger ionic radius, the average ionic radius of A-site $<r_A>$ increase with the increasing of the Sr concentration from 1.179 A^0 for x = 0 to 1.221 A^0 for x = 0.32 in $Pr_{0.68}Ca_{0.32-x}Sr_xMnO_3$ alloy. As concluded in Ref. [27], due to the increase in $<r_A>$, the Mn-O-Mn bond angle distortion decreases and consequently the electron bandwidth (W) increases and hence the hopping amplitude for the electrons in the e_g bond becomes larger causing reduction in resistance with the increase of Sr content. The increase in Mn-O-Mn bond angle and hence the electron bandwidth stabilize the FM state by increasing the DE interaction and consequently FM fraction of the sample increases. This is also because an increase in MI transition temperature (T_{MI}) with the increase of Sr content. It is known that the magnetization of the PS manganites is strongly dependent on the applied magnetic fields. In the PS region, the application of a magnetic field leads to a metamagnetic transition by increasing the FM volume. This behavior induces a huge resistance variation and MR ratio, though to be related to the percolation of the FM phase that forms electrical paths where the resistance decreases several orders of magnitude [23].

At low temperature ($T < T_{MI}$) the metallic behavior of the samples can be explained in terms of electron-electron, electron-magnon and electron-phonon scattering of the carriers. In order to understand the transport mechanism of $Pr_{0.68}Ca_{0.32-x}Sr_xMnO_3$ samples, we have fitted the love temperature resistance data with the following expression

$$\rho = \rho_0 + \rho_{2.5} T^{2.5} \qquad (1)$$

where ρ_0 term represents the resistance arises from domain, grain boundary and other temperature independent effects. The second term $\rho_{2.5}$ denotes the electron-magnon scattering contribution [27, 39]. As can be seen from Eq. 1, the electron-magnon scattering contribution is predominant in low temperature regime. The values of ρ_0 and $\rho_{2.5}$ are obtained from fitting the resistance curves (Fig 1) with Eq.1 are given in Table 1. It is clearly seen that the values of both ρ_0 and $\rho_{2.5}$ decrease with increase of x. As discussed in our previous study [8], the PS $Pr_{0.65}Ca_{0.35-x}Sr_xMnO_3$ has spatially coexisting FM metallic and CO-AFM insulating regions. The substitution of Ca^{2+} with the bigger Sr^{2+} ions provokes an increase of $<r_A>$ and hence magnetic properties of the system could changes from CO –AFM insulating to fully FM metallic state. Due to the increase in FM metallic phase with increasing x, the size of the domain boundary decreases and hence ρ_0 becomes smaller. The decrease of $\rho_{2.5}$ with x could be explained as suppression of structural disorder. As concluded above, the substitution of Ca by larger Sr ions decreases the Mn-O-Mn bond angle distortion and consequently electron bandwidth (W) increases. The increase in W causes a considerable decrease in spin fluctuations and electron-magnon scattering and consequently $\rho_{2.5}$ becomes smaller.

Table 1. Model parameters obtained from fitting the resistance data of $Pr_{0.68}Ca_{0.32-x}Sr_xMnO_3$ with $\rho = \rho_0 + \rho_{2.5}T^{2.5}$

x	ρ_0 (Ω)	$\rho_{2.5}$ ($\Omega K^{-2.5}$)
0.18	0.18	2.610×10^{-6}
0.26	0.06	0.344×10^{-6}
0.32	0.04	0.140×10^{-6}

In the high temperature ($T > T_{MI}$) insulating region the conductivity is dominated by the thermally activated hopping of small polarons. In order to understand the transport mechanism of $Pr_{0.68}Ca_{0.32-x}Sr_xMnO_3$ samples in high temperatures, the resistance data are fitted with small polaron hopping model which has the form [27, 40]

$$\rho(T) = A\,T \exp\left(\frac{E_a}{k_B T}\right) \qquad (2)$$

where k_B is Boltzmann constant and E_a is the activation energy. In this study, Eq.(2) is used to fit the resistance curves above T_{MI}. The activation energy E_a is calculated from the fitting process of the linear portion of the $\ln(\rho/T)$-T^{-1} curves (Fig. 3). The results are given in Table 2. It is clearly seen that the activation energy decreases with the increase of Sr content (x) (Fig. 4). This result clearly suggests that the effective height of the polaron hopping barrier decrease in Sr doped $Pr_{0.68}Ca_{0.32-x}Sr_xMnO_3$ system which could be caused by decrease of Mn-O-Mn bond angle distortions. This should also increase the number of effective charge carrier in the Sr doped systems. The inset of Fig. 4 presents the variation of activation energy as a function of magnetic field for x = 0.1 sample. It is clear that the activation energy decreases with the increase of magnetic field as similar to the increase of Sr concentration (x). Similar trend is also observed in other samples of the series. As reported in Ref. [27] and [31], the role of increasing Sr concentration (x) and magnetic field are the same for delocalization of charge carriers and spin ordering in the $Pr_{0.68}Ca_{0.32-x}Sr_xMnO_3$ system.

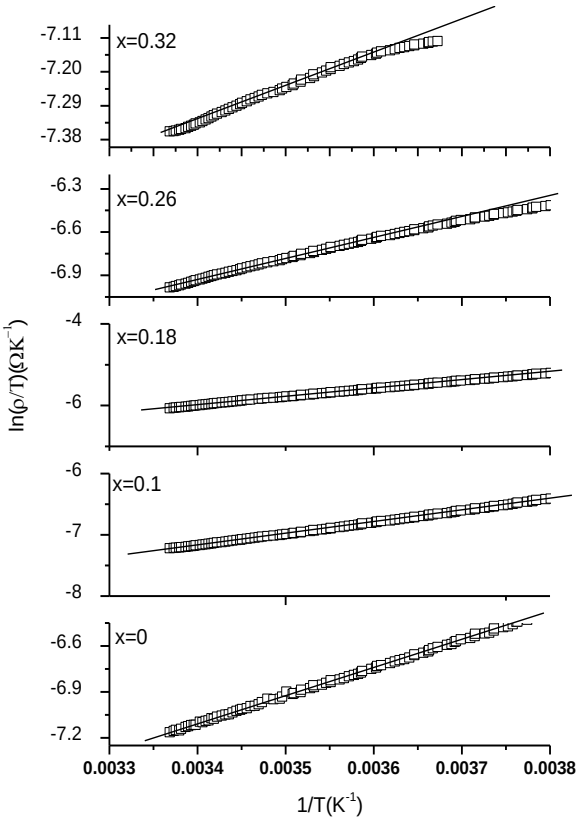

Fig. 3. Variation of ln(ρ/T) as a function of inverse temperature for x = 0, 0.1, 0.18, 0.26 and 0.32 samples.

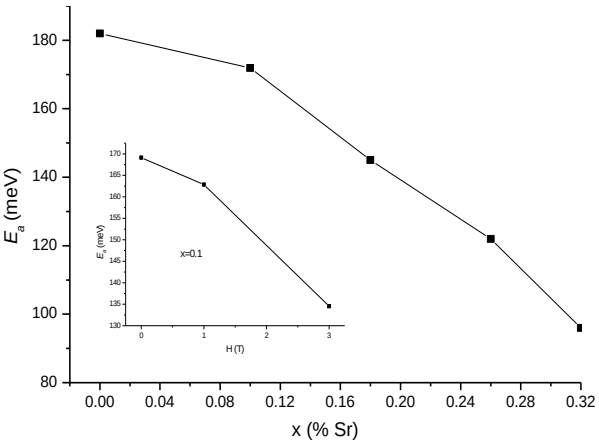

Fig. 4.The variation of activation energy (Ea) as a function of x. The inset presents the variation of Ea as a function of magnetic field for x =0.1 sample.

Table 2. Metal-insulator temperatures and parameters for small polaron hopping conduction of $Pr_{0.68}Ca_{0.32-x}Sr_xMnO_3$

x	T_{MI} (K)	E_a (meV)	A ($x10^{-5}$)
0	---	182.16	0.0514
0.1	---	171.93	0.0602
0.18	218	145.17	1.174
0.26	254	122.28	1.275
0.32	280	96.65	1.512

The MR ratio, defined as MR(%) = 100x[R(0)-R(H)]/R(H) where R(0) and R(H) are the resistance at zero and at H magnetic fields respectively, was measured as a function of the magnetic field up to 6 T at various temperatures from 5 to 300 K. Fig.5 and Fig 6 show the MR ratio for x = 0 and 0.1 samples at various temperatures. It is clearly seen that due to the coexistence of FM metallic and CO insulating phases for the samples x = 0 and 0.1 an unusual anomaly is observed in MR curves. The MR ratio of $6.3x10^8$ for x =0 at 60 K and $4.3x10^5$ for x = 0.1 at 100 K in a 6 T magnetic field are one of the largest MR reported for $Pr_{0.68}Ca_{0.32-x}Sr_xMnO_3$ alloys especially in polycrystalline form. This may be due to a particular unstable mixing phase of a weak CO insulating at high temperatures and a FM metallic phase at low temperatures. Therefore, the application of a low magnetic field is enough to partially melt the CO phase and percolate the FM state to enhance the metallic property. Hence, the large enhancement of MR indicates its electronic and magnetic instability or PS below its T_{MI} at low magnetic fields. Fig. 7, 8 and 9 show the MR ratio of the samples for x = 0.18, 0.26 and 0.32 respectively. As can be seen, the maximum MR decreases considerably with increasing Sr content (from 279% for x =0.18 to 100% for x =0.32 near the T_{MI} transition temperatures and in a 6 T magnetic field). This indicates that the introduction of Sr atoms reduces the MR values. As concluded above, Sr substitution can modify the electronic, magnetic and transport properties of $Pr_{0.68}Ca_{0.32-x}Sr_xMnO_3$ by increasing the average ionic radius of A-site $<r_A>$ and consequence decreases the magnitude of MR. If the resistance curves of $Pr_{0.68}Ca_{0.22}Sr_{0.1}MnO_3$ and $Pr_{0.68}Sr_{0.32}MnO_3$ (Fig.2 a and e) are compared with each other, it is clearly seen that the resistance ratio of $Pr_{0.68}Ca_{0.22}Sr_{0.1}MnO_3$ decreases rapidly with increase of magnetic fields while that of $Pr_{0.68}Sr_{0.32}MnO_3$ changes very little. This may be explained as the $Pr_{0.68}Ca_{0.22}Sr_{0.1}MnO_3$ exposes mixture of FM metallic and CO insulating phases. As the magnetic field increase, the size of FM domains increases and hence resistance is considerably decreases which cause a huge MR ratio. In the case of large Sr concentration rate, due to the more stable metallic behavior the MR considerably decreases with increasing Sr content.

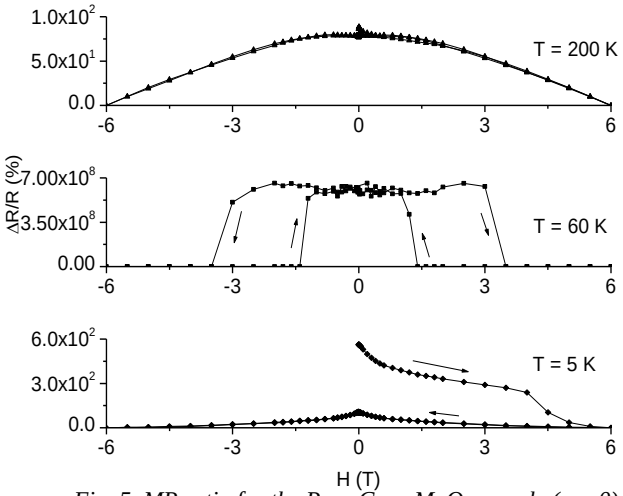

Fig. 5. MR ratio for the $Pr_{0.68}Ca_{0.32}MnO_3$ sample (x = 0) at various temperatures.

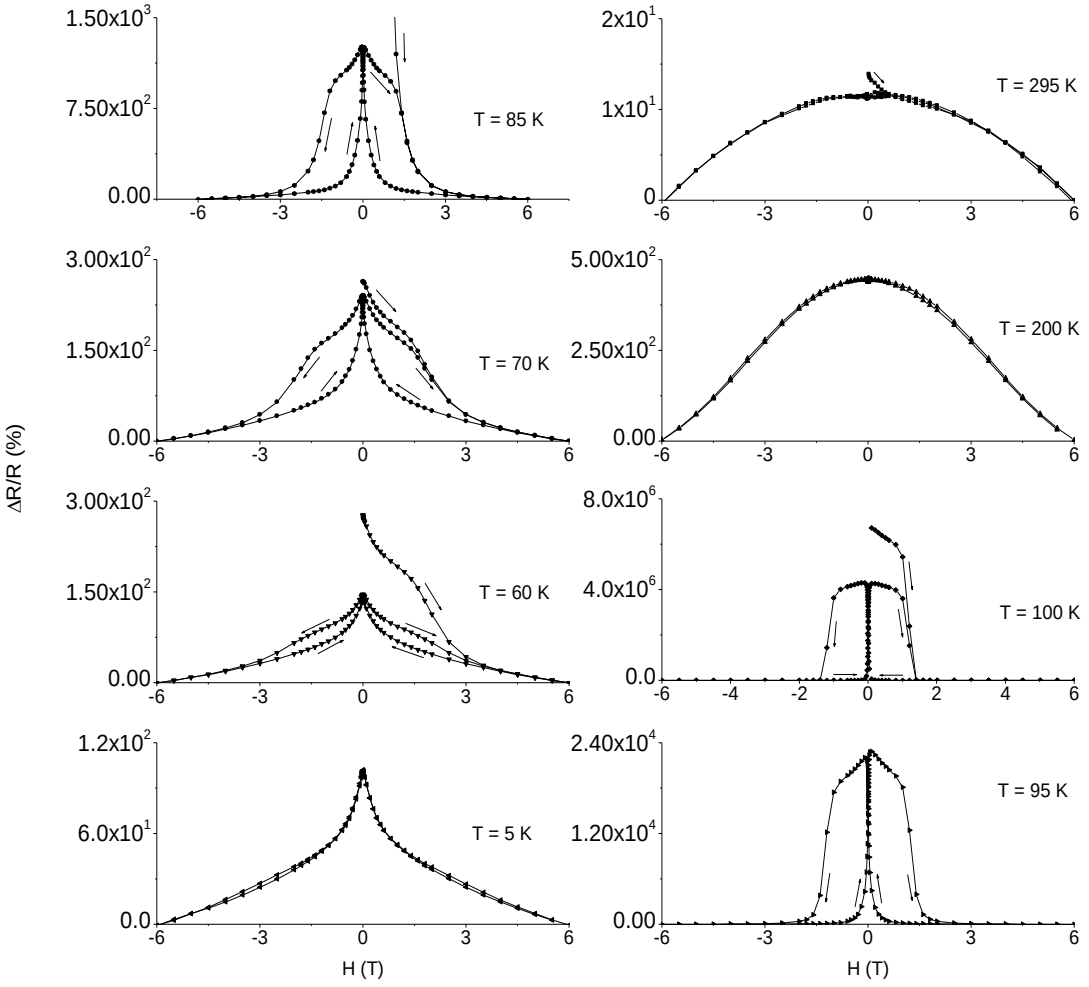

Fig. 6. MR ratio for the $Pr_{0.68}Ca_{0.22}Sr_{0.1}MnO3$ sample (x = 0.1) at various temperatures.

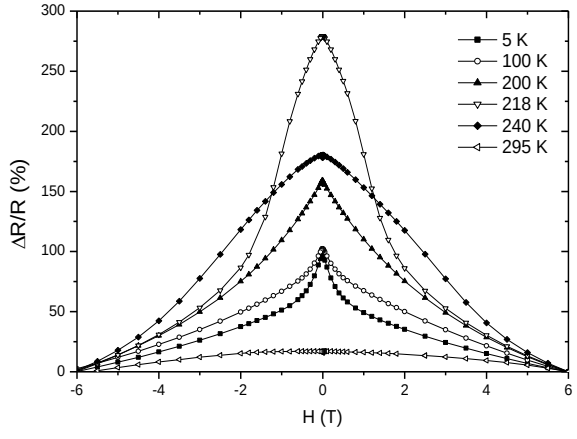

Fig. 7. MR ratio for the $Pr_{0.68}Ca_{0.14}Sr_{0.18}MnO3$ sample (x = 0.18) at various temperatures.

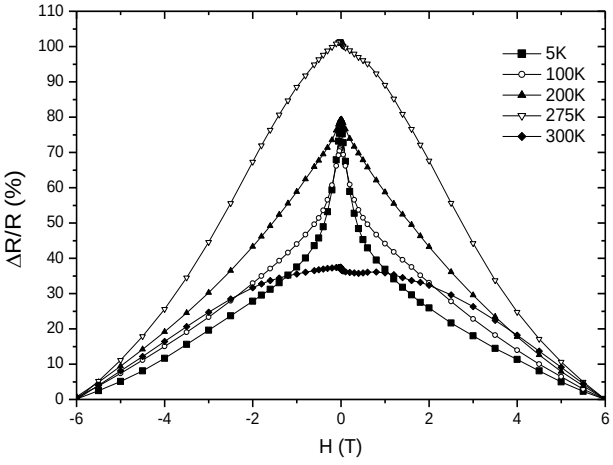

Fig. 8. MR ratio for the $Pr_{0.68}Ca_{0.06}Sr_{0.26}MnO3$ sample (x = 0.26) at various temperatures.

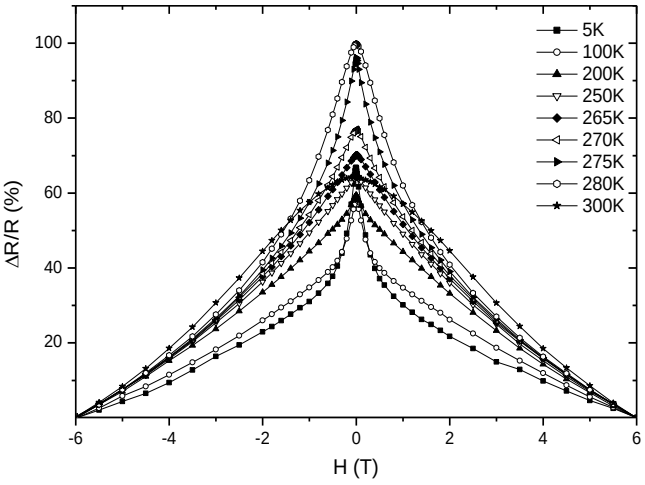

Fig. 9. MR ratio for the $Pr_{0.68}Sr_{0.32}MnO3$ sample (x = 0.32) at various temperatures.

4. Conclusions

In this work, the magnetotransport and magnetoresistance properties of $Pr_{0.68}Ca_{0.32-x}Sr_xMnO_3$ (x= 0, 0.1, 0.18, 0.26 and 0.32) compounds were investigated. The resistance curves indicated that the system presents an evolution from a charge-ordered manganite at x = 0; with an insulating-like resistivity and low magnetization values, towards to a completely ferromagnetic metallic state for x = 0.32. Below T_{MI}, domain, grain boundary and electron-magnon scattering contribution to the resistance were investigated. It was found that both the domain, grain boundary and electron-magnon scattering contributions decreased with increasing Sr content. Above T_{MI}, the resistance curves were fitted to the small polaron popping model. The activation energy (E_a) was found to decrease with increasing Sr content.

In the intermediate (phase separated) region, due to the coexistence of FM metallic and CO insulating phases the MR was found to be maximum. The MR ratio of $6.3x10^8$ for x =0 at 60 K and $4.3x10^5$ for x = 0.1 at 100 K in a 6 T magnetic field are one of the largest MR value reported for $Pr_{0.68}Ca_{0.32-x}Sr_xMnO_3$ alloys especially in polycrystalline form. The MR decreases considerably with increasing Sr content (from 279% for x =0.18 to 100% for x =0.32). Sr substitution can modify the electronic, magnetic and transport properties of $Pr_{0.68}Ca0._{32-x}Sr_xMnO_3$ by increasing the average ionic radius of A-site $<r_A>$ and consequence decreases the MR values.

This detailed study indicates that the substitution of Sr in $PrCaMnO_3$ manganites has a great influence on transport properties and magnitude of magnetoresistance properties.

Acknowledgements

This work was supported by Inonu University research fund with the project number 2010/09.

References

[1] H. Roder, J. Zhang, A. R. Bishop, Phys. Rev. Lett. **76**, 1356 (1996).
[2] V.K. Pecharsky, K.A.Gschneider, Phys.Rev.Lett. **78**, 4494 (1997).
[3] H. Gencer, S. Atalay , H.I. Adiguzel, V.S. Kolat, Physica B **357**, 326 **(**2005).
[4] V.S. Kolat, H. Gencer, S. Atalay, Physica B **371** 199 (2006).
[5] H. Gencer, V.S. Kolat, S. Atalay, J. Alloys and Comp. **422**, 40 **(**2006).
[6] V.S. Kolat, H. Gencer, M. Gunes, S. Atalay, Mat.Scien. and Eng. B **140**, 212 (2007).
[7] M.H. Phan, S.C. Yu, J.Magn.Magn.Mater. **308**, 325 **(**2007).
[8] V.S.Kolat, T. İzgi, A.O. Kaya, H.Gencer, N. Bayri, S.Atalay, J. Magn. Magn. Mater. **322**, 427 (2010).
[9] S. Jin, T.H. Tiefel, M. McCormack, R.A.Fastnacht, R.Ramesh, C.H. Chen, Science **264**, 413 **(**1994).
[10] R.V. Holmolt, J. Wocker, B. Holzapfel, L. Schultz, K. Samwer, Phys. Rev. Lett. **71**, 2331 (1993).
[11] A.P. Ramirez, J. Phys.: Condens. Matter. **9**, 8171 **(**1997).
[12] C.Zenner, Phys.Rev. **82**, 403 (1951).
[13] W.J. Li, B. Zhang, W. Lu, Y.P. Sun, Y. Zhang, J. Phys. And Chem. of Solids, **68**, 1749 (2007).
[14] H.Y. Hwang, S.W. Cheong, P.G. Radaeli, M. Marezio, B. Batlogg, Phys. Rev. Lett. **77**, 914 (1995).
[15] R. Mathieu, Y. Tokura, J. Phys. Soc. Jpn. **76**, 124706 **(**2007) .
[16] M.Y. Kagan, A.V. Klaptsov, I.V. Brodsky, K.I. Kugel, A.O. Sboychakov, A.L. Rakhmanov, J. Phys. A: Math. Gen. **36**, 9155 **(**2003).
[17] E. Dagotto, Phys.Rep. **344,** 1 **(**2001).
[18] D. Niebieskikwiat, R.D. Sanchez, A. Caneiro, J. Magn. Magn. Mater. **237**, 241 **(**2001).
[19] Q. Huang, J.W.Lynn, R.W. Erwin, A. Santoro, D.C. Dender, V.N. Smolyaninova, K. Ghosh, R.L. Grene, Phys. Rev. B **61**, 8895 (2000).
[20] M.M.Savosta, A.S. Karnachev, S. Krupicka, J. Hejtmanek, Z. Jirak, M. Marysko, P. Novak, Phys. Rev. B **62**, 545 **(**2000).
[21] N. Fukumoto, S. Mori, N. Yamamoto, Y. Moritomo, T. Katsufuji, C.H. Chen, S.W. Cheong, Phys. Rev. B **60**, 12963 **(**1999).
[22] R. Mahendiran, M.R. Ibarra, A. Maignan, F. Millange, A. Arulraj, R. Mahesh, B. Raveau, C.N.R. Rao, Phys. Rev. Lett. **82**, 2191 **(**1999).
[23] M. Uehara, S. Mori, C.H. Chen, S.W.Cheong, Nature **399**, 560 **(**1999).
[24] Y. Tomioka, A.Asamitsu, Y. Moritomo, H. Kuwahara, Y. Tokura, Phys. Rev. Lett. **74**, 5108 (1995).
[25] C. Martin, A. Maignan, M. Herview, B. Raveau, Phys. Rev. B **60**, 12191 **(**1999).
[26] D. Niebieskikwiat, R.D. Sanchez, A.J. Caneiro, J. Magn. Magn. Mater. **237**, 241 **(**2001).

[27] S. Mollah, H.L. Huang, H.D.Yang, S.Pal, S. Taran, B.K. Chaudhuri, J. Magn. Magn. Mater. **284**, 383 **(**2004).
[28] J. Wu, H. Zheng, J.F.Mitchell, C.J Leighton, J. Magn. Magn. Mater. **288**, 146 (2005).
[29] D.C. Krishna, P.V. Reddy, J. Alloys and Comp. **479**, 661 (2009).
[30] S. Mollah, H.L. Huang, H.D.Yang, Mat. Lett. **611**, 2329 (2007).
[31] Y. Tomioka, A. Asamitsu, H. Kuwahara, Y.J. Tokura, J. Phys. Soc. Jpn. 66, 302 (1997).
[32] A. Maignan, C.Simon, V.Caignaert, B.Raveau, Solid State Commun. **96**, 623 (1995).
[33] J. Hejtmanek, Z. Jirak, D. Sedmidubsky, A. Maignan, C. Simon, V. Caignaert, C. Martin, B. Raveau, Phys. Rev. B **54**, 11947 **(**1996).
[34] S. Mollah, H.L. Huang, P.L. Ho, W.L. Huang, C.W. Huang, C.P Sun, J.Y. Lin, S.J. Liu, Y.S. Gou, W.H.Li, H.D.Yang, J. Magn. Magn. Mater. **265**, 215 (2003).
[35] S. Mollah, C.P. Sun, H.L. Huang, P.L. Ho, H.D. Yang, J. Appl. Phys. **95**, 6813 (2004).
[36] H. Liu, Y. Luo and M. Li, Physica B **395**, 33 (2007).
[37] M. Roy, J.F. Mittchell, A. Ramirez, P. Schiffer, Phil. Magazine B **81**, 417 **(**2001).
[38] X.X. Zhang, J. Tejeda, Y. Xin, G.F. Sun, K.W. Wong, X. Bohigas, Appl. Phys. Lett. **69**, 3596 (1996).
[39] S. Taran, S. Karmakar, H. Chou, B. K. Chaudhuri, Phys. Stat. Sol. (b) **243** , 1853 (2006).
[40] W. S. Khan,S. K. Hasanain, Phys. Scr. **81**, 065702 (2010).

*Corresponding author: hgencer@inonu.edu.tr